

2 Design of ligands for the human VASP EVH1 domain

The EVH1 domain of the human protein VASP binds the consensus sequence motif FPxφP [25]. The natural interaction partners for VASP include the proteins zyxin and vinculin. A more strongly binding natural ligand can be found in the surface protein ActA of the pathogenic bacterium *Listeria monocytogenes* [26]. The binding motif occurs four times in this protein [27], in close tandem repeat. The most strongly binding sequence is SFEFPPPTEDEL [25]. This peptide has an affinity of 45 μM as determined by NMR titration measurements (data shown below). A substitution analysis with natural amino acids has been performed using the SPOT technique, resulting in the grid shown in Figure 4 [25]:

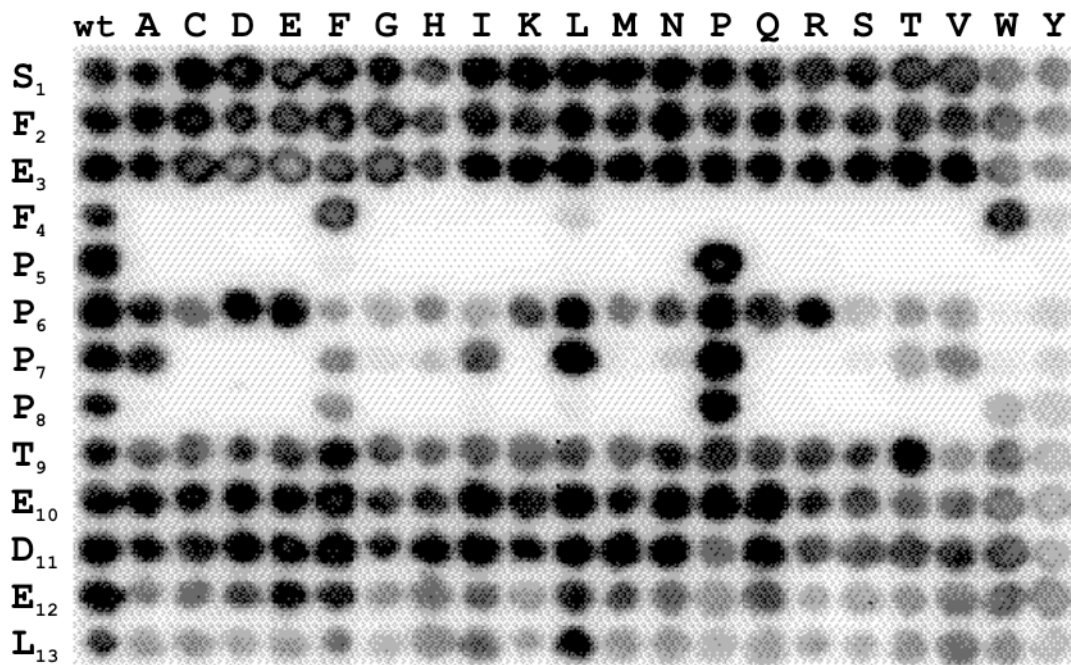


Figure 4
SPOT scan of VASP EVH1: Single substitution analysis of the ActA peptide; each amino acid in the peptide was substituted in turn against all natural amino acids. Peptides were synthesized on a cellulose membrane. Each spot represents a point mutation. Detection of chemiluminescence was performed by incubation with GST-EVH1, a primary GST antibody from rabbit and a secondary anti-rabbit antibody linked to horse raddish peroxidase. The figure shows the negative image. (See Materials and Methods for details).

The proline residue in position 5 can clearly not be substituted for any other natural amino acid. The Phe residue in position 4 can only be substituted by Trp. The proline residue in position 8 can only be substituted for an aromatic residue (Phe or Trp), or for Val, with weak retention of binding. Pro in position 6 is comparatively unspecific and may be substituted by any other natural amino

acid with moderate to strong retention of binding. Pro 7 can only be substituted by hydrophobic amino acids [25].

The aim of the present study was the development of new ligands incorporating peptoidic building blocks in those positions of the ActA peptide that cannot or only with dramatic loss of affinity be substituted with a natural amino acid. Such peptomeric compounds are less susceptible to proteolysis and are of interest both in research concerning the role of VASP in cells and whole organisms as well as being potential lead structures for drug development. While similar approaches have been used for SH3- and WW-domains[20, 28], no ligands have been designed for EVH1 domains before.

2.1 Design of a peptomer library

The general structure of peptoidic residues as opposed to a natural amino acid is shown in Figure 5. A peptoidic residue bears a sidechain on the backbone nitrogen atom and two hydrogen atoms on $C\alpha$.

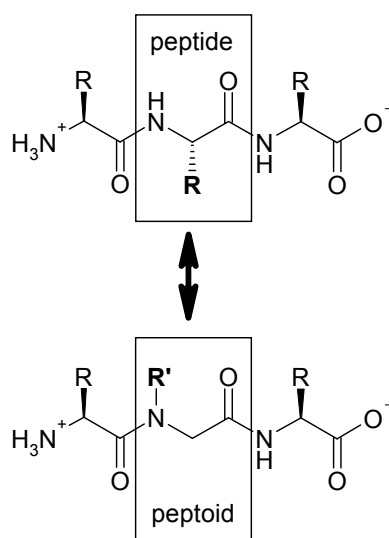


Figure 5
Structure of a peptide residue vs. a peptoid residue. Amines used to introduce the moiety R' are depicted in Table 1, p. 21. The synthesis follows the reaction scheme outlined in Scheme 3.2, p. 71.

For the study presented here 24 primary amines were chosen that were converted into the peptoid sidechain R' during the synthetic process. These covered a broad range of chemical properties from hydrophilic to hydrophobic and aromatic. The structures are summarized in Table 1.

In order to elucidate the binding properties when substituting residues F₂, F₄, P₅, P₈ and L₁₃ of the ActA derived peptide with peptoidic residues comprised of these amines, a new SPOT scan was performed. Residues were substituted one by one for the 24 possible peptomeric structures. For the two Pro residues P₅ and P₈ a twodimensional grid was constructed, including all possible combinations of the 24 building blocks. This grid is shown if Figure 6.

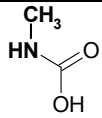

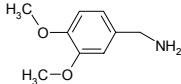
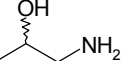
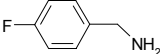
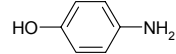
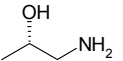
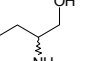
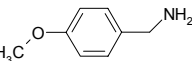
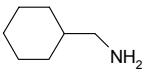
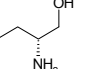
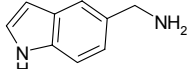
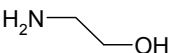
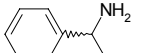
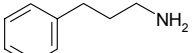
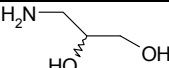
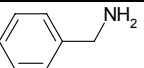
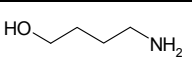
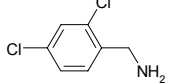
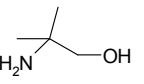
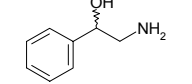
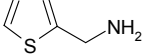
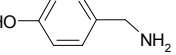
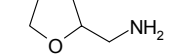
Nr.	Peptoid building block	Nr.	Peptoid building block	Nr.	Peptoid building block
1*		9		17	
2		10		18	
3		11		19	
4		12		20	
5		13		21	
6		14		22	
7		15		23	
8		16		24	

Table 1
Primary amines used to introduce R' (see Figure 5) in the synthesis of peptomers.
The amine group of each compound was transformed into the backbone amide of a peptoid residue in the synthetic process. The reaction is outlined in Materials and Methods, page 71.

* Sarcosine, corresponding to methylamine, was used in the Fmoc protected form.

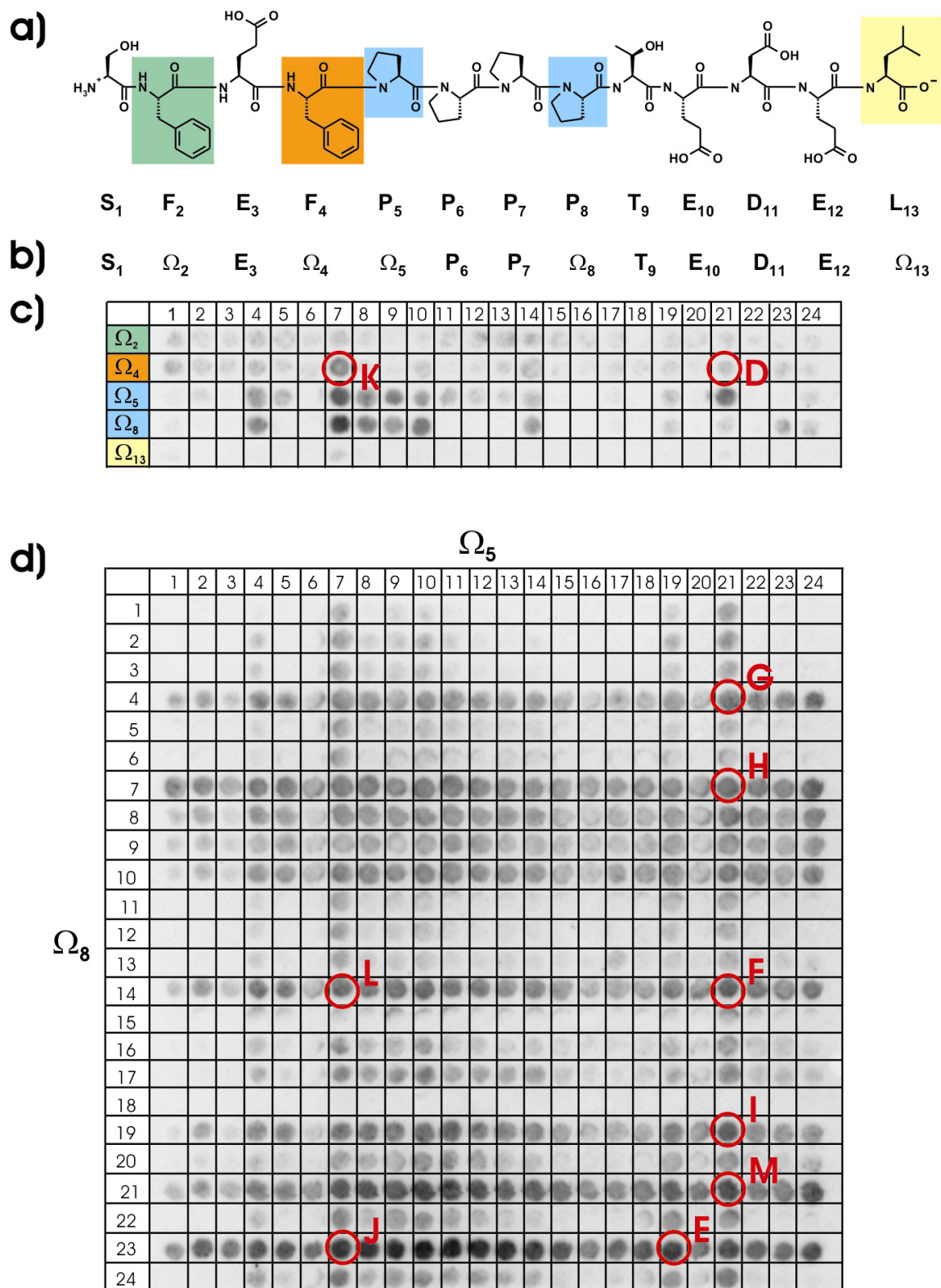


Figure 6 Substitution analysis of the peptide ligand from ActA (SFEFPPPTEDEL) known to bind the VASP EVH1 domain. *a)* Structure and sequence of the ActA ligand. Conserved residues chosen for substitution are highlighted. *b)* Residues that were substituted by peptoid building blocks are denoted with Ω *c)* Results of the single substitution of peptide residues 2, 4, 5, 8 and 13 using the 24 amines shown in Table 1. *d)* Results of simultaneous, double substitution of peptide residues P_5 and P_8 . Numbers 1 to 24 at the border of the grid correspond to numbers in Table 1; letters D to M within the grid correspond to the peptomers shown in Table 2. (Although shown in two parts in this figure, the analysis was carried out on one membrane, incubated in one piece. Digital processing of the image was performed for the whole grid.)

Part a) of the figure shows the structure of the ActA peptide. Highlighted are the residues under investigation. Single substitutions of each of these residues are shown in panel b). No binding of the VASP EVH1 domain is observed for any substituent in position L₁₃, which apparently cannot be substituted using these peptoid building blocks, indicating the importance of leucine at this position. It has been pointed out in the literature that the terminal EL residues of the peptide are highly important for the overall binding affinity of the peptide [25]. Similar observations can be made for F₂, which is also not amenable to substitution with any of the peptoid building blocks used.

Single substitutions of F₄ for peptoid building block 7 (see Table 1), P₅ for peptoid building blocks 4, 7-10 and 21, and P₈ for peptoid building blocks 4, 7-10, 14 and 23, all resulted in peptomers which bound to the VASP EVH1 domain as judged from the SPOT analysis.

When substituting both P₅ and P₈ simultaneously, the SPOT scan shown in panel c) is obtained. Both of the conserved proline residues investigated, P₅ and P₈, could be readily substituted by several of the peptoid building blocks in Table 1 without loss of EVH1 binding ability, as was already seen from the single substitution analysis. Not surprisingly, hydrophobic substituents are favoured, as these two prolines are known to pack tightly into a hydrophobic groove on the EVH1 domain surface [29]. Interestingly, the two proline residues do not show identical behaviour, highlighting differences due to the asymmetry of the FPxϕP:EVH1 interface. P₅ appears to be more tolerant to a wider range of the substituents than P₈, but in general both positions require hydrophobic sidechain groups similar to those of the natural proline. In the case of peptoid building block 9, the long aliphatic chain has the conformational freedom to fold back onto itself and fill the hydrophobic pocket normally occupied by the proline. Peptoid building block 21 was very well tolerated in place of P₅ but not in place of P₈. The three carbon aliphatic chain of this peptoid building block provides sufficient flexibility to allow the ring to bend around into the position normally occupied by the P₅ pyrrolidine sidechain.

Given a "good" substitution for P₈ most other sidechains are tolerated at P₅ while maintaining EVH1-binding. The most strongly VASP EVH1-binding doubly-substituted peptomers were those for which P₈ was replaced by peptoid blocks 4, 7-10, 14, 19, 21 or 23, and P₅ replaced by peptoid building blocks 7 or 21. This choice was based on the intensity of spots on the membrane. As was seen later, the intensity of spots correlates only moderately well with binding affinities in this study. From these data, ten of the apparently strongly EVH1-binding peptomers (circled in red in Figures 6.b and 6.c and labelled D to M in table 2) were selected for quantitative measurements of EVH1-binding affinity.

2.2 Binding studies of peptomer ligands by Biacore

Milligram quantities of the peptides A-C (Table 2) and each of the ten peptomers, D-M were synthesized using classical solid support peptide chemistry with appropriate modifications for the incorporation of peptoid building blocks (see Chapter 5). Binding affinities to the VASP EVH1 domain were measured using the Biacore technique.

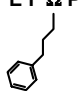
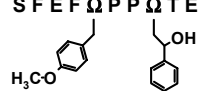
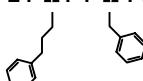
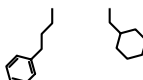
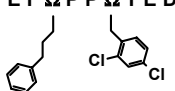
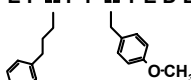
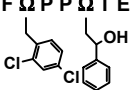
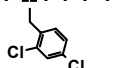
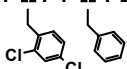
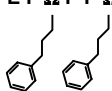
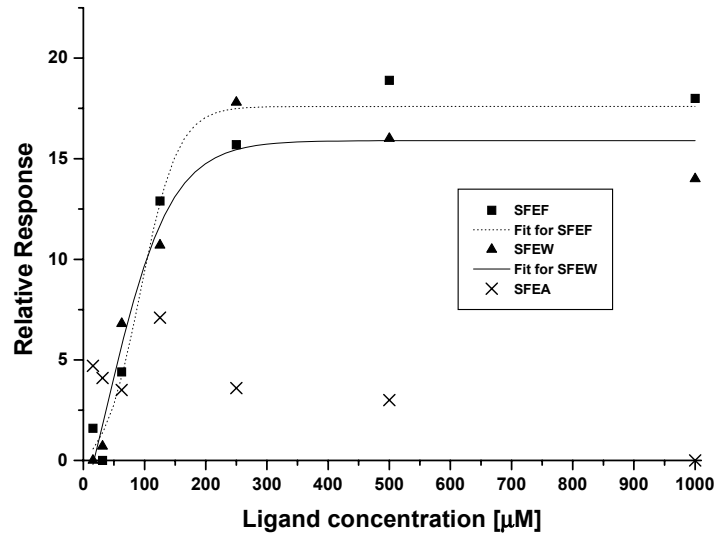
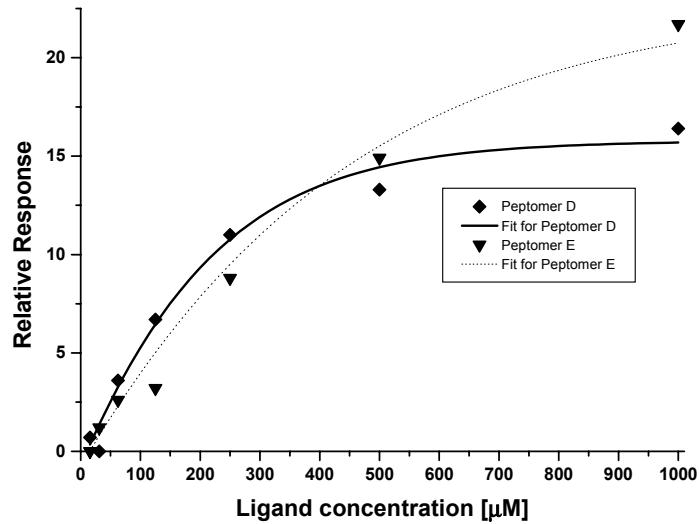
Peptide/ Peptomer	Structure	K _D [μM]	
		Biacore	NMR
A	SFEFPPPTEDEL	55.1	45.0
B	SFEAPPPTEDEL	-*	-*
C	SFEWPPPTEDEL	13.7	n.d.
D	SFEFΩPPPTTEDEL 	120.4	90.0
E	SFEFΩPPΩTEDEL 	250.3	250.0
F	SFEFΩPPΩTEDEL 	381.9	
G	SFEFΩPPΩTEDEL 	410.6	
H	SFEFΩPPΩTEDEL 	455.3	
I	SFEFΩPPΩTEDEL 	508.5	
J	SFEFΩPPΩTEDEL 	842.9	
K	SFEFΩPPPTTEDEL 	995.7	
L	SFEFΩPPΩTEDEL 	1,215.1	
M	SFEFΩPPΩTEDEL 	1,694.8	

Table 2 The affinity of three peptides (Wild type peptide (A) and two mutants using natural amino acids, B and C) and 10 peptomers (letters D to M, compare Figure 3) to the VASP EVH1 domain were determined by Biacore and NMR spectroscopy. Ω represents a peptoid residue.



a)



b)

Figure 7

Binding curves resulting from Biacore measurements.

Panel a) shows curves for the natural peptide SFEFPPPTEDEL, as well as for the mutants SFEW... and SFEA...

Panel b) shows results for the two most strongly binding peptomers D and E.

The measured affinities varied over a relatively wide range from 45 μM to 1.7 mM. It should be noted that it was clearly possible to distinguish between weak and non-binding ligands (e.g. SFEA...) based on the distribution of points on the respective plots. All N-substituted peptomers showed weaker EVH1-binding than the wild type ActA peptide SFEFPPPTEDEL and its natural amino acid derivative SFEWPPPTEDEL. The Biacore measurements showed that peptomer D possesses the strongest EVH1-binding affinity (K_D 120.4 μM), with peptomer E the second best,

already binding more weakly by a factor of 2 (K_D 250 μ M). Peptomers F to K all bound with K_D 's less than 350 μ M, whereas L and M showed only very weak association with the EVH1 domain.

2.3 Binding studies of peptomers by NMR: Chemical shift mapping

Based on the results of the Biacore measurements, peptomers D and E were chosen for more detailed studies using NMR chemical shift titrations. Figure 8 shows the overlaid 2D 15 N-HSQC spectra acquired at the beginning and end of a titration of the 15 N labelled EVH1 domain with peptomer D.

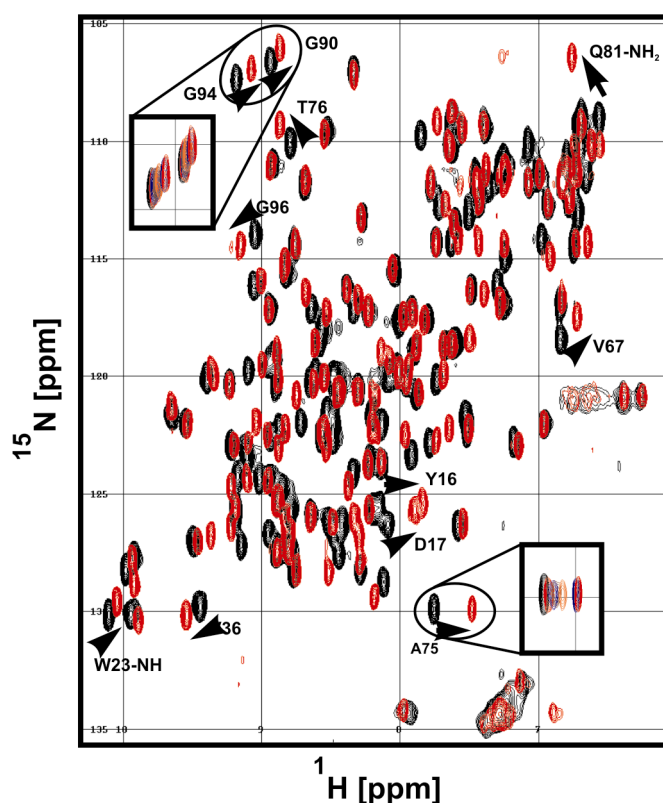


Figure 8
Titration of EVH1 with peptomer D. The initial spectrum without ligand is shown in black, the spectrum with a ten times molar excess of ligand is shown in red. Magnifications show the most pronounced changes in the spectrum through all titration steps. Arrows point at some residues exhibiting strong changes in their corresponding peak positions. The protein concentration was 0.1 mM. Assignments used in this study were kindly provided by Linda J. Ball and are given in Appendix 6.1.1.

The stepwise addition of the peptomer gave rise to continuous changes in the 15 N and 1 H chemical shifts of EVH1 domain residues involved in ligand binding, as exemplified for residues A₇₅, G₉₀

and G₉₄. The total ¹⁵N-¹H chemical shift perturbations (CSPs) were combined and weighted according to $\Delta\delta_{\text{TOTAL}} = \Delta\delta(^1\text{H}) + 0.2*\Delta\delta(^{15}\text{N})$ in order to scale the chemical shift values of ¹⁵N relative to ¹H [30]. These were then plotted against the ligand concentration for peptide A and peptomers D and E to calculate the binding constants shown in Figure 9 (also listed in Table 2). The K_D values obtained from NMR titrations correlated reasonably well with those obtained from Biacore measurements for each of the ligands studied.

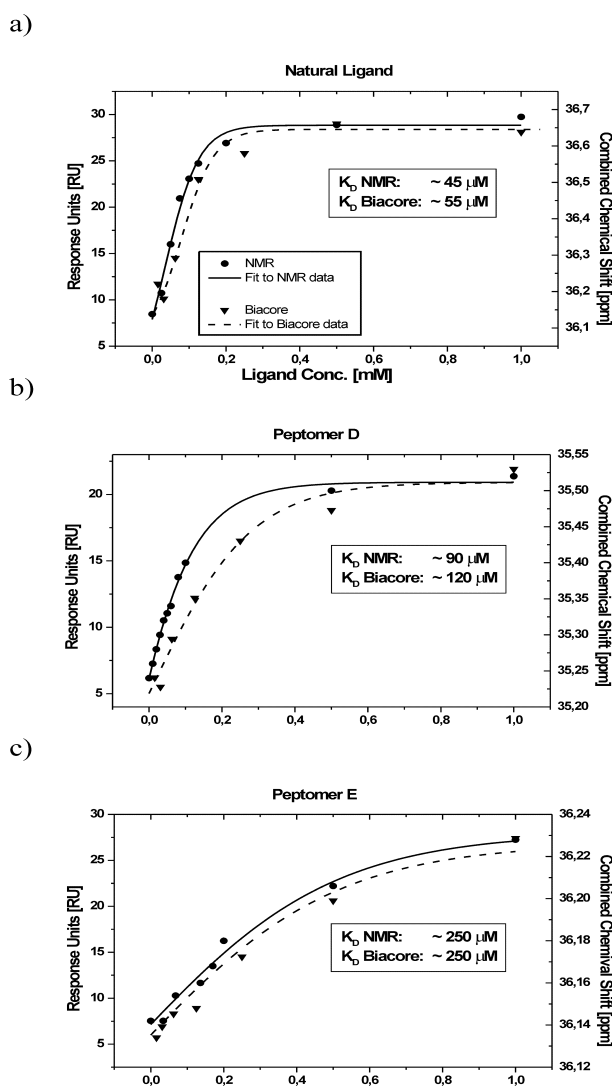


Figure 9
Titration results of EVH1 with the ActA ligand and peptomers D and E. Protein concentration in all NMR measurements was 0,1 mM. Residue Ala 75 was chosen for these curves.

The distribution of perturbed shifts in the EVH1 sequence is shown in Figure 10 for the three ligands studied. The overall pattern of EVH1 residues perturbed due to binding of peptomers D and E is similar to the pattern observed for EVH1 binding to the *Listeria* ActA peptide. Not surprisingly, the more weakly binding peptomer E causes generally weaker CSPs.

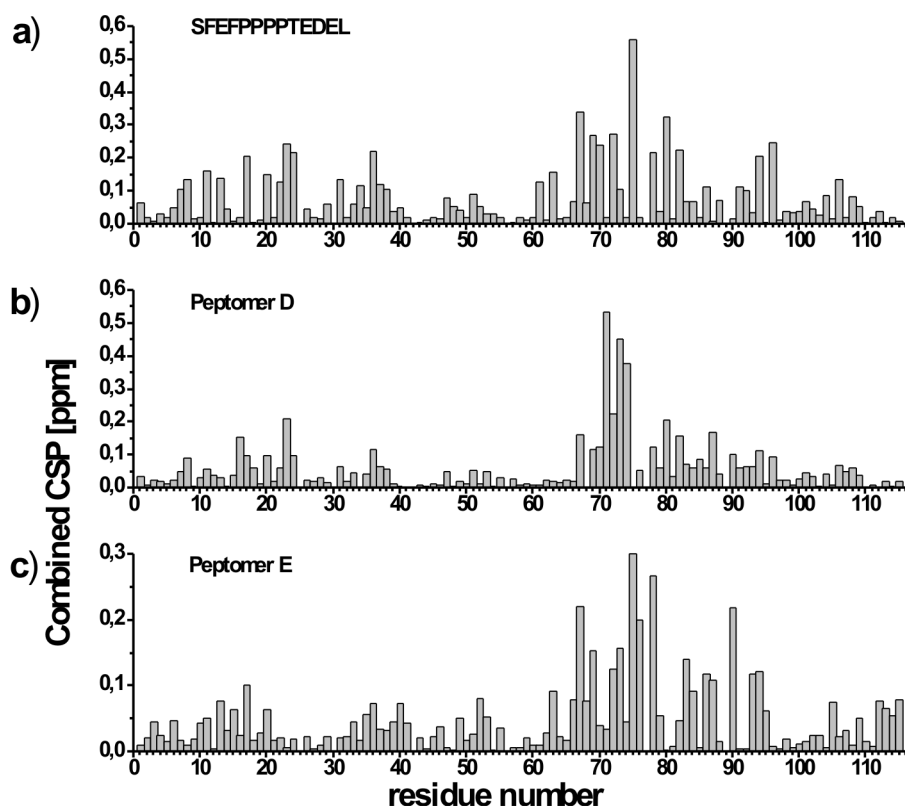


Figure 10
 Changes in backbone NH Chemical Shift between pure protein and ten times molar excess of respective ligand. CSP has been calculated as $\Delta\delta_{\text{TOTAL}} = \Delta\delta(^1\text{H}) + 0.2 \cdot \Delta\delta(^{15}\text{N})$. The y-axis for plot c) is extended for clarity.

The most pronounced changes occur in the region between residues 70 and 75 of EVH1. This corresponds to β -strand 5, which forms part of the EVH1 binding interface. The region around Trp 23 is also affected. The sidechain NH group of this Trp forms a crucial H-bond to the carbonyl group of ligand P₆, as described for the umbrella model in the introduction.

2.4 Models of Binding and Ligand Design

The CSP pattern was used as a qualitative basis for molecular modelling of EVH1 in complex with peptomer D. The modelling study was performed by Ronald Kühne. The model of the complex formed with peptomer D, in which P₅ was replaced with peptomer block 21, is shown in Figure 11. In peptomer D, the N-substituted residue replacing P₅ contains an aromatic sidechain separated from the backbone by a three-carbon aliphatic linker. This provides a sufficient degree of flexibility to enable the linker methylene groups to occupy the P₅ pocket without steric hindrance from the sidechain of F₄, which in the model is located in its usual hydrophobic groove in the EVH1 domain

surface [25, 29, 31]. This shows that P₅ can be replaced by a peptoid building block with a large N-substituted sidechain maintaining EVH1 affinity.

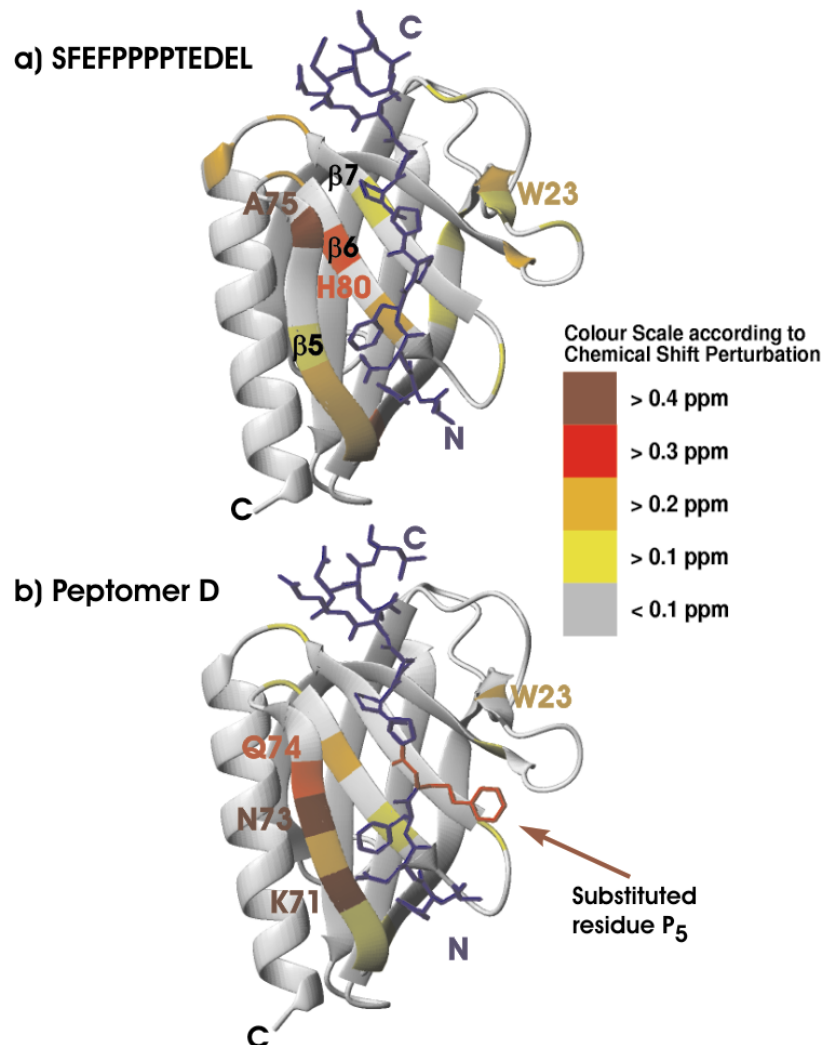


Figure 11
a) Structure of EVH1 in complex with the ActA ligand [25]
b) Model of the complex between EVH1 and peptomer D, based on observed CSP. Mapped on the EVH1 domain are the most pronounced shift changes for backbone amide NH-groups.

Close inspection of the model showed the N-substituted sidechain to be in close enough proximity to the F₄ binding site that, in the absence of F₄, this new ring could occupy the F₄ binding pocket. If this was the case it should be possible to design an EVH1-binding peptomer in which the normally essential F₄ sidechain was replaced with a much smaller alternative sidechain on condition that a neighbouring N-substituted sidechain could occupy the F₄ binding pocket. To test this hypothesis, peptomer N was synthesized, an analogue of peptomer D with the residue F₄ substituted for Ala. The absence of the large F₄ sidechain should now allow the N-substituted sidechain unhindered access to the F₄ binding pocket.

A titration with peptomer N gave the CSP as shown in Figure 12:

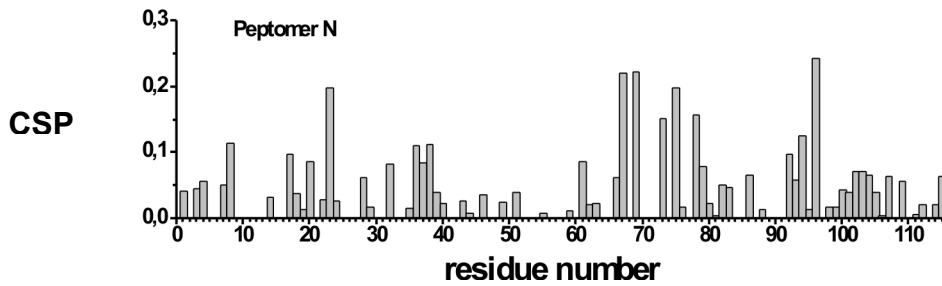


Figure 12
Changes in backbone NH Chemical Shift between pure protein and ten times excess of peptomer N.

The observed CSPs were generally weak and comparable in magnitude to those seen for peptomer E. A pronounced change occurs for Trp 23, showing that similar interactions occur as for the complex with the ActA peptide. β -strand 5 is again affected. Based on this pattern a model was delineated as above, shown in Figure 13.

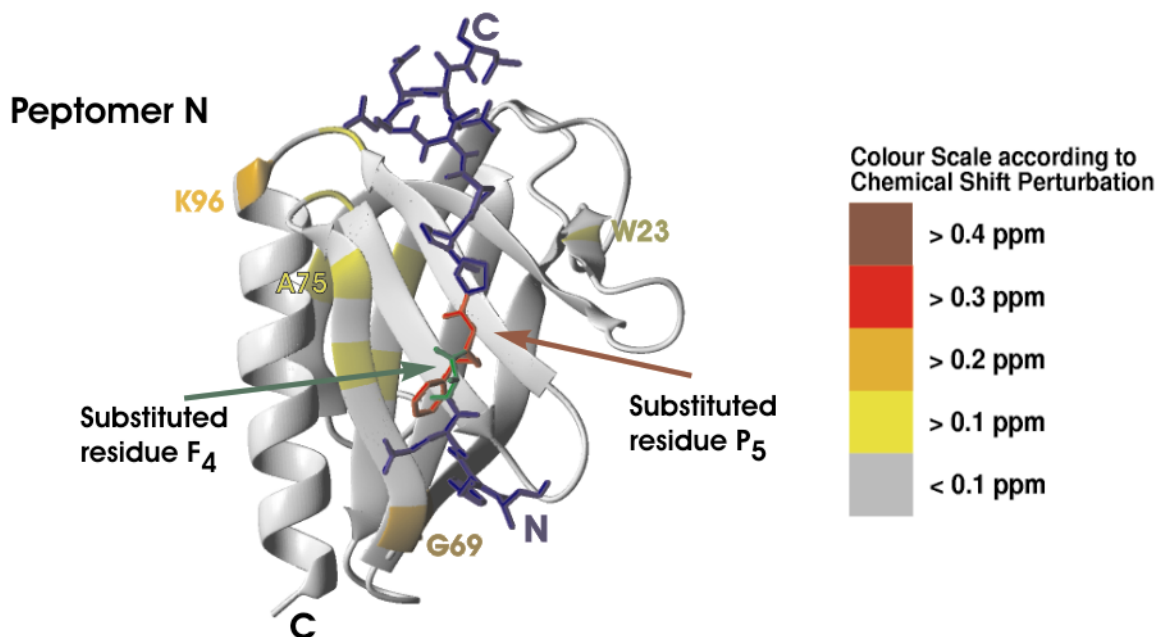


Figure 13
Model of the complex between EVH1 and peptomer N, based on observed CSP. Mapped on the EVH1 domain are the most pronounced shift changes for backbone amide NH-groups.

The sidechain of position 5 is located in the F₄ binding site without disruption of binding contacts of the remaining parts of the ligand. This positioning seems reasonable, since there are no shift changes in the neighbouring loop formed by residues 83 to 87. Changes in that part of the protein were observed for peptomer D.

By designing a ligand capable of occupying the known F₄ binding pocket, the usually essential F₄ residue could be substituted. A titration was performed in order to determine the affinity of peptomer N to EVH1 (Figure 14).

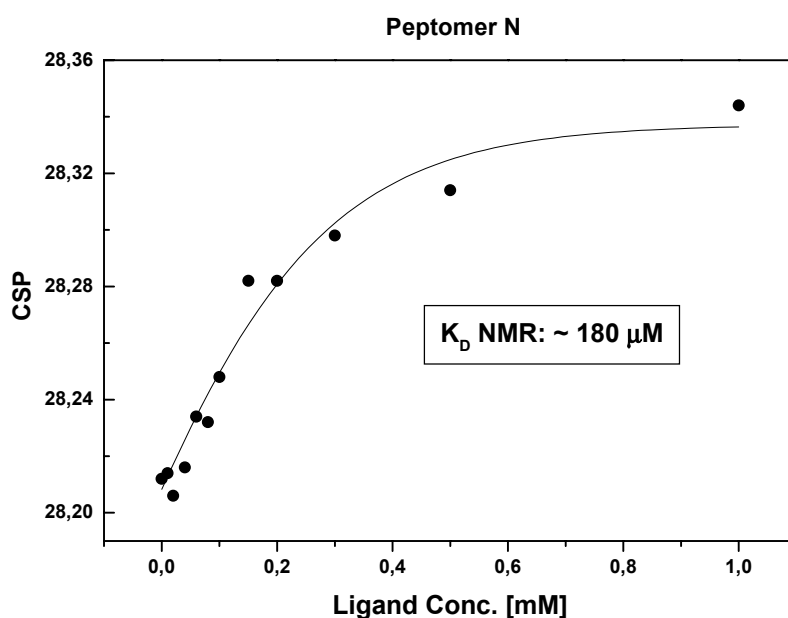


Figure 14
Titration of EVH1 with peptomer N. Protein concentration was 0,1 mM.

The K_D value of peptomer N was $\sim 180 \mu\text{M}$, approximately a factor of four weaker than the ActA peptide and a factor of two weaker than peptomer D. This is the first example of an EVH1 ligand where both residue F₄ and residue P₅ have been substituted simultaneously while maintaining affinity to the domain.

Figure 15 shows the differences in CSPs in response to the addition of peptomer N. These differences are localized in specific regions of the protein which make contacts to those sidechains in the ligand which were substituted. The difference in CSP between SFEFPPPTEDEL and Peptomer D and between Peptomer D and Peptomer N are shown in Figures 15.a and 15.b, respectively. The most pronounced CSP differences cluster to residues in the β -sheet comprising strands β_5 – β_6 – β_7 which is involved in binding of the natural ligand.

The subtracted CSPs in Figure 15.b show the effects of the F₄A substitution in the ligand. Again, the region from residues 70-74 shows the most drastic changes as this is the region of the EVH1 domain which forms the closest contacts to F₄. According to our model (Figure 11), binding to the substituted ligand causes a small re-orientation of the sheet β_5 – β_6 – β_7 . Residue K96, at the beginning of the α -helix, also shows a considerable CSP which is probably due to small

movements of the helix in response to the reorientation of the adjacent β -sheet. As observed for peptomer D, Tyr 16 and Trp 23 are again weakly perturbed, indicating small changes in the interactions of the recognition triad (Ball et al. *Angewandte Chemie International Edition* 2004, in press).

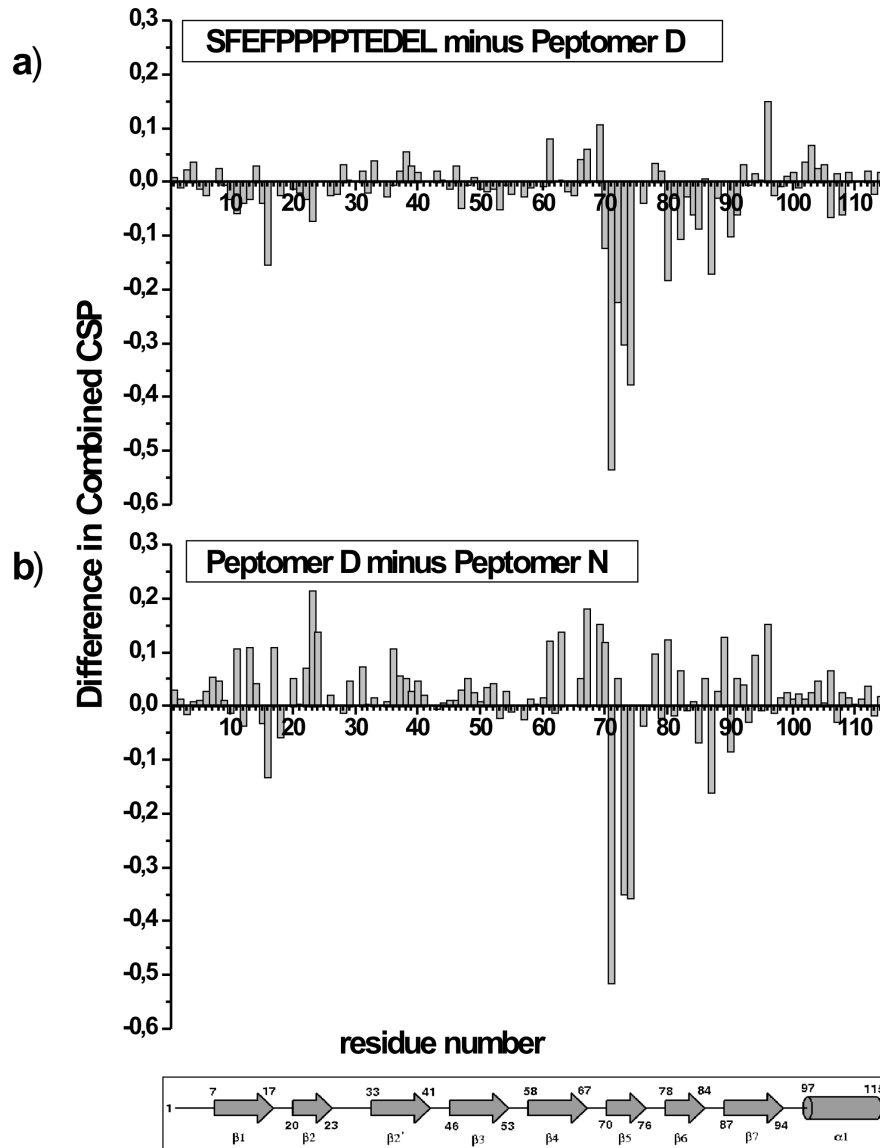


Figure 15
Differences between titration of the ActA peptide and peptomer D, and peptomers D and N.

The structure of the ActA peptide in complex with EVH1 and the two models for the complexes with peptomers D and N were compared and the differences in $C\alpha$ positions measured, shown in Figure 16.

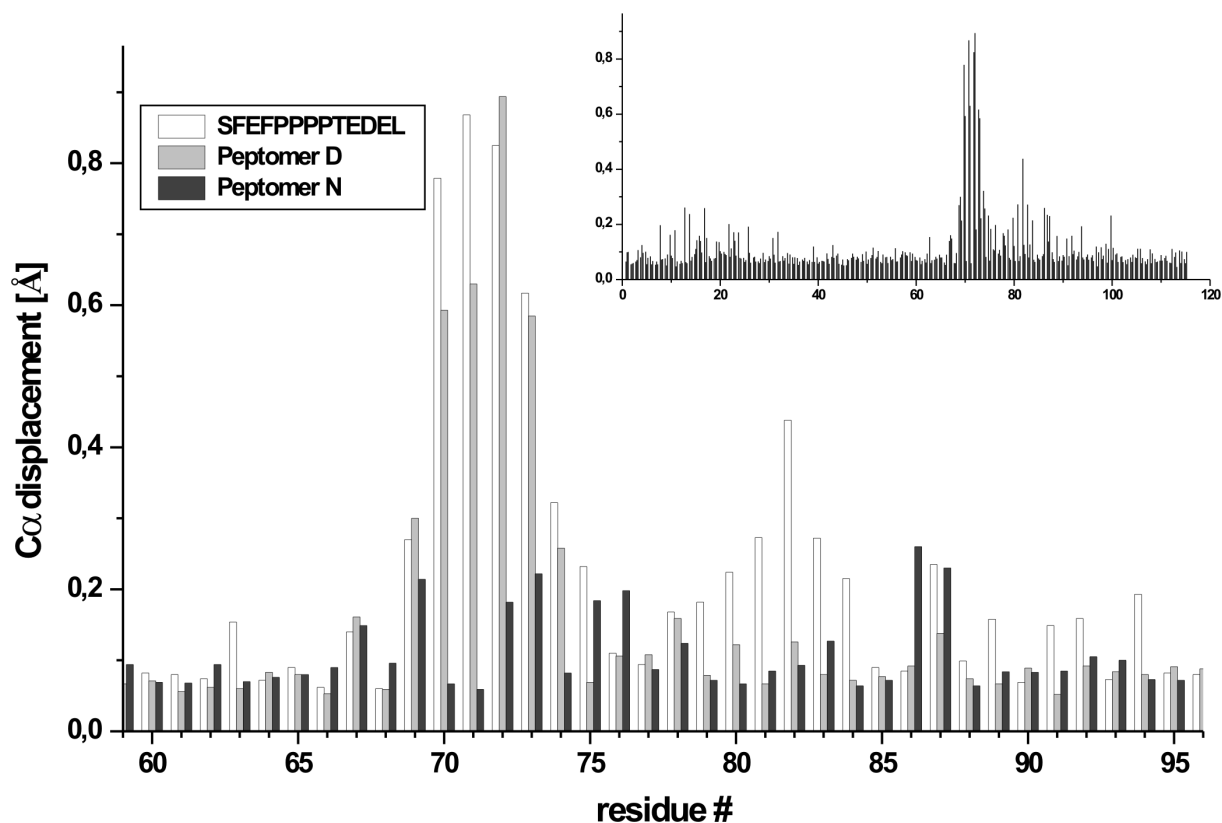


Figure 16
Change in C α position of the three complexes relative to the free protein. The inset shows the whole domain, enlarged are β -strands 4, 5, 6 and 7. As observed for CSP, the changes cluster in β -strand 5.

The C α displacement was biggest for residues 71-75 of β 5, residues 80-84 of β 6, and residues 86 and 87 in the centre of β 7. The displacement is most pronounced in these regions for the natural peptide and peptomer D. Peptomer N shows differences suggesting a more native-like conformation of the domain when bound. This may be due to weaker contacts in the F₄ binding region due to incomplete or sub-optimal occupation of the F₄ binding pocket.

In an attempt to calculate a structure for the complex of the VASP EVH1 domain with peptomer N, rather than calculating a model, a 1:10 molar ratio complex of uniformly $\{^2\text{H}, ^{15}\text{N}\}$ -labelled EVH1 domain with the unlabelled peptomer in 90% $\text{H}_2\text{O}/10\%\text{D}_2\text{O}$ was prepared and a 3D ^{15}N -edited NOESY spectrum was measured. Any NOEs seen in the aliphatic or aromatic regions of the indirect proton dimension to the ^{15}N -attached protons detected in this experiment should therefore be exclusively intermolecular between protein and ligand. However, no such intermolecular NOEs were detected in these experiments, probably due to the weakness of the NOE transfer from such a weakly binding ligand (180 μM).

2.5 Discussion

This work underlines the importance of gaining an understanding of the detailed interactions of protein domains with their natural ligands from high resolution structural data and shows how this information can be used to explain the conservation of specific residues on domain surfaces, which are not involved in stabilization of the fold. Once it is understood why certain properties are conserved, the natural ligands can be modified to design new ligands in which specific positions are exchanged for non-natural building blocks without abolishing binding ability. One long term aim of this work would be to design ligands with desired binding affinities already in mind. Ligands with stronger binding affinities than the natural partners could be used as highly specific small-molecule modulators for reversibly tuning and conditionally perturbing chosen protein interactions on time-scales not possible with other genetic techniques [32].

This could be important for the Ena/VASP proteins to which dual modes of function in both facilitation and inhibition of actin-based processes have been repeatedly assigned, depending on whether sub-cellular or cellular functions have been studied in different cell types [33, 34]. New ligands of this type may open a way for the selective modulation of EVH1 domain interactions with their respective binding partners *in vitro* and *in vivo*. These compounds are only in part peptidic and hence are less prone to proteolytic cleavage *in vivo*. As has been observed for mice, salvage pathways for the function of VASP exist in many cell types. Therefore it appears feasible to use VASP ligands like these in the treatment of diseases that involve pathologically altered cell adhesion or cell motility while maintaining the natural body functions via salvage pathways.